21

Actuators and Computer-Aided Design of Robots

Miomir Vukobratović
Mihajlo Pupin Institute

Veljko Potkonjak
University of Belgrade

Kenji Inoue
Osaka University

Masaharu Takano
Kansai University

At the beginning of a discussion on robot design one should recall the history of robotics. During the early stage of robotics, no exact theory existed to assist engineers in designing robots. The designers followed the rich experience of machine building. In the 1970s, the theory of robotics started to grow fast. At the same time, industry manufactured and implemented rather complex robots capable of solving many industrial tasks. However, there was little connection between theory and industrial practice. The theory of robots was too academic. The problems considered were often too advanced for the industrial robotics of that time. Theoretical research dealt with mathematical modeling of robot dynamics, problems of control of nonlinear multivariable systems like robots, stability of control, even force feedback, etc. It seems that robot industry did not believe the need for some exact theory.

Experience in machine building and control represented sufficient background for design of many successful robots. Presently, the necessity for complex, precise, and high-speed robots requires a close connection between theory and practice. Regarding the application of robot dynamics, the main break-through was made when computer-aided methods for dynamic modeling were developed (see Chapter 20). Such methods allowed fast and user-friendly calculation of all relevant dynamic effects. It became possible to examine the a robot's behavior in advance, that is before it was actually built. A mathematical model replaced the real system. Such simulation was relevant depending on the quality of the model. In the beginning, the models were restricted to open-type linkages. Links were considered infinitely rigid and joints frictionless. In spite of these approximations, the dynamic model covered the main effects, inertial behavior of the spatial robotic system. Later, other relevant effects were included as explained in Section 20.5.

If a simulation system based on dynamic model is supplemented with appropriate testing of the dynamic characteristics and the user-friendly interface for changing robot parameters, one obtains

a very useful design tool. A designer can examine the influence of certain parameters to robot performance and then change the parameters to improve the results. In this way, step by step, he or she approaches the optimal design. Finally, it is possible to create a software system that includes optimization procedures, thus automating the choice of robot parameters. This is a brief idea of something called computer-aided design (CAD).[1,16]

When selecting the topics for this chapter devoted to robot design we started from the fact that technology grows fast. Thus, some currently advanced constructive solutions might soon become obsolete. Hence, we decided to avoid presentation of specific constructive solutions and try to explain advanced principles of robot design. First, it was necessary to discuss robot-driving systems. It is important because the choice of actuator type (electric, hydraulic, or pneumatic) is one of the first decisions in the design process and many constructive solutions depend on this choice. Also, dynamic models of actuators are needed for knowledge of overall robot dynamics and to create the simulation system. Actuators and their impact to robot design are discussed in Section 21.1; Section 21.2 gives the principles of advanced design. A CAD system for industrial robots is described.

21.1 Robot Driving Systems

Discussion on robot-driving systems is important for several reasons. First, we address the problem of dynamic modeling. The actuators represent a subsystem of the entire robot. It is often said that a robot consists of a mechanical part (robot mechanism) and actuators. For mathematical modeling of robot dynamics it is necessary to take care of all dynamic effects, those introduced by the mechanism (e.g., link inertia) and those due to actuators (e.g., rotor inertia, counter electromotive forces, etc.).[1,2] Such a model of the complete dynamics is derived in Sections 21.3.1 and 21.3.2.

The problem of control is strongly influenced by the choice of actuators. For instance, DC motors, stepper motors, and hydraulic actuators require different hardware and software solutions. The problem of control is closely related to the driving characteristics of different types of actuators. Finally, constructive solutions of the robot's mechanical part depend on the choice of actuators. For instance, if a hydraulic cylinder drives a robot elbow, it is attached to the upperarm and the forearm, representing a kind of direct drive. On the other hand, if a DC motor is used, it is usually displaced from the elbow and located on the robot base. This concept understands a mechanism for transmitting motor power to the joint.

So, when elaborating robot actuators it is necessary to stress the following points: operation principles, mathematical modeling, driving characteristics, and mounting on the robot arm. Section 21.1.1 presents a review of actuators currently used in robots and automation. The main characteristics, advantages, and drawbacks are mentioned without detailed explanation. The idea is to stress those points that are important for implementation. In the paragraphs that follow we discuss the principles of operation and the mathematical description of most common types of actuators. Some constructive aspects of actuator implementation are also considered (especially the transmission). Presentation covers DC motors, hydraulic actuators, and pneumatic drive.

21.1.1 Present State and Prospects

In the early stage of robotics, pneumatic cylinders were often used to drive the manipulation mechanisms. Such devices had limited motion possibilities. This follows from the binary character of pneumatic actuators. The piston can extend to the final position or retract to the initial state and no control is achieved between these two positions. This is due to the compressibility of the air that flows through the cylinder. Thus, the manipulator can reach a set of points in space and programming of motion means only the definition of the sequence of working points. Although some special designs of pneumatic drives offer the possibility of achieving closed-loop control, such actuators are not widely used in advanced robotic systems. However, there is still a need for

pick-and-place industrial systems positioned by mechanical stops. For such devices pneumatic actuation represents a fast, cheap, and reliable solution.

The hydraulic actuator is to some extent similar to the pneumatic one but avoids its main drawbacks. The uncompressible hydraulic oil flows through a cylinder and applies pressure to the piston. This pressure force causes motion of the robot joint. Control of motion is achieved by regulating the oil flow. The device used to regulate the flow is called a servovalve. Hydraulic systems can produce linear or rotary actuation. There are many advantages of the hydraulic drives. Its main benefit is the possibility of producing a very large force (or torque) without using geartrains. At the same time, the effector attached to the robot arm allows high concentration of power within small dimensions and weight. This is due to the fact that some massive parts of the actuator, like the pump and the oil reservoir, are placed beside the robot and do not load the arm. With hydraulic drives it is possible to achieve continuous motion control. The drawbacks one should mention are:

Hydraulic power supply is inefficient in terms of energy consumption
Leakage problem is present.
A fast-response servovalve is expensive.
If the complete hydraulic system is considered (reservoir, pump, cylinder and valve), the power supply becomes bulky.

Electric motors (electromagnetic actuators) are the most common type of actuators in robots today. They are used even for heavy robots for which some years ago hydraulics was exclusive. This can be justified by the general conclusion that electric drives are easy to control by means of a computer. This is especially the case with DC motors. However, it is necessary to mention some drawbacks of electromagnetic actuation. Today, motors still rotate at rather high speed. Rated speed is typically 3000 to 5000 r.p.m. At the same time, the output motor torque is small compared with the value needed to move a robot joint. For instance, rated torque for a 250W DC motor with rare-earth magnets may be 0.9 Nm. Hence, electric motors are in most cases followed by a reducer (gear-box), a transmission element that reduces speed and increases torque. It is not uncommon for a large reduction ratio to be needed (up to 300). The always present friction in gear-boxes produces loss of energy. The efficiency (output to input power ratio) of a typical reducer, the Harmonic Drive, is about 0.75. The next problem is backlash that has a negative influence on robot position accuracy. Similar problems may arise from the unsatisfactory stiffness of the transmission.

An important question concerns the allocation of the motor on the robot arm. To unload the arm and achieve better static balance, motors are usually displaced from the joints they drive. Motors are moved toward the robot base. In such cases, additional transmission is needed between the motor and the corresponding joint. Different types of shafts, chains, belts, ball screws, and linkage structures may be used. The questions of efficiency, backlash, and stiffness are posed again. Finally, the presence of transmission elements makes the entire structure more complex and expensive. This main disadvantage of electric motors can be eliminated if direct drive is applied. This understands motors powerful enough to operate without gearboxes or other types of transmission. Such motors are located directly in the robot joints. Direct drive motors are used in advanced robots, but not very often. Problems arise if high torques are needed. However, direct drive is a relatively new and very promising concept.[5]

The most widely used electromagnetic drive is the permanent magnet DC motor. Classical motor structure has a rotor with wire windings and a stator with permanent magnets and includes brush-commutation. There are several forms of rotors. A cylindrical rotor with iron has high inertia and slow dynamic response. An ironless rotor consists of a copper conductor enclosed in a epoxy glass cup or disk. A cup-shaped rotor retains the cylindrical-shaped motor while the disc-shaped rotor allows short overall motor length. This might be of importance when designing a robot arm. A disadvantage of ironless armature motors is that rotors have low thermal capacity. As a result, motors have rigid duty cycle limitations or require forced-air cooling when driven at high torque

levels. Permanent magnets strongly influence the overall efficiency of motors. Low-cost motors use ceramic (ferrite) magnets. Advanced motors use rare-earth (samarium-cobalt and neodymium-boron) magnets. They can produce higher peak torques because they can accept large currents without demagnetization. Such motors are generally smaller in size (better power to weight ratio). However, large currents cause increased brush wear and rapid motor heating.

The main drawback of the classical structure comes from commutation. Graphite brushes and a copper bar commutator introduce friction, sparking, and the wear of commutating parts. Sparking is one of the factors that limits motor driving capability. It limits the current at high rotation speed and thus high torques are only possible at low speed. These disadvantages can be avoided if wire windings are placed on the stator and permanent magnets on the rotor. Electronic commutation replaces the brushes and copper bar commutator and supplies the commutated voltage (rectangular or trapezoidal shape of signal). Such motors are called brushless DC motors. Sometimes, the term synchronous AC motor is used although a difference exists (as will be explained later). In addition to avoiding commutation problems, increased reliability and improved thermal capacity are achieved. On the other hand, brushless motors require more complex and expensive control systems. Sensors and switching circuitry are needed for electronic commutation.

The synchronous AC motor differs from the brushless DC motor only in the supply. While the electronic commutator of a brushless DC motor supplies a trapezoidal AC signal, the control unit of an AC synchronous motor supplies a sinusoidal signal. For this reason, many books and catalogues do not differentiate between these two types of motors.

Inductive AC motors (cage motors) are not common in robots. They are cheap, robust, and reliable, and at the same time offer good torque characteristics. However, control of such motors is rather complicated. Advanced vector controllers are expensive and do not guarantee the same quality of servo-operation as DC motors. Still, it should be pointed out that these motors should be regarded as prospective driving systems. The price of controllers has a tendency to decrease and control precision is being improved constantly. Presently, cage AC motors are used for automated guided vehicles, and for different devices in manufacturing automation.

Stepper motors are often used in low-cost robots. Their main characteristic is discretized motion. Each move consists of a number of elementary steps. The magnitude of the elementary step (the smallest possible move) depends on the motor design solution. The hardware and software needed to control the motor are relatively simple. This is because these motors are typically run in an open-loop configuration. In this mode the position is not reliable if the motor works under high load — the motor may loose steps. This can be avoided by applying a closed-loop control scheme, but at a higher price.

Let us now discuss some ideas for robot drives that are still the topic of research. First, we notice that all the discussed actuators can be described as kinematic pairs of the fifth class, i.e., pairs that have one degree of freedom (DOF). Accordingly, such an actuator drives a robot joint that also has one DOF. This means that multi-DOF joints must not appear in robots, or they have to be passive. If a multi-DOF connection is needed, it is designed as a series of one-DOF joints. However, with advanced robots it would be very convenient if true multi-DOF joints could be utilized. As an example, one may consider humanoid robots that really need spherical joints (for shoulder and hip). To achieve the possibility of driving a true spherical joint one needs an actuation element that could be called an artificial muscle. It should be long, thin, and flexible. Its main feature would be the ability to control contraction. Although there have been many varying approaches to this problem (hydraulics, pneumatics, materials that change the length in a magnetic field or in contact with acids, etc.), the applicable solution is still missing.

21.1.2 DC Motors: Principles and Mathematics

DC motors are based on the well-known physical phenomenon that a force acting upon a conductor with the current flow appears if this conductor is placed in a magnetic field. Hence, a magnetic

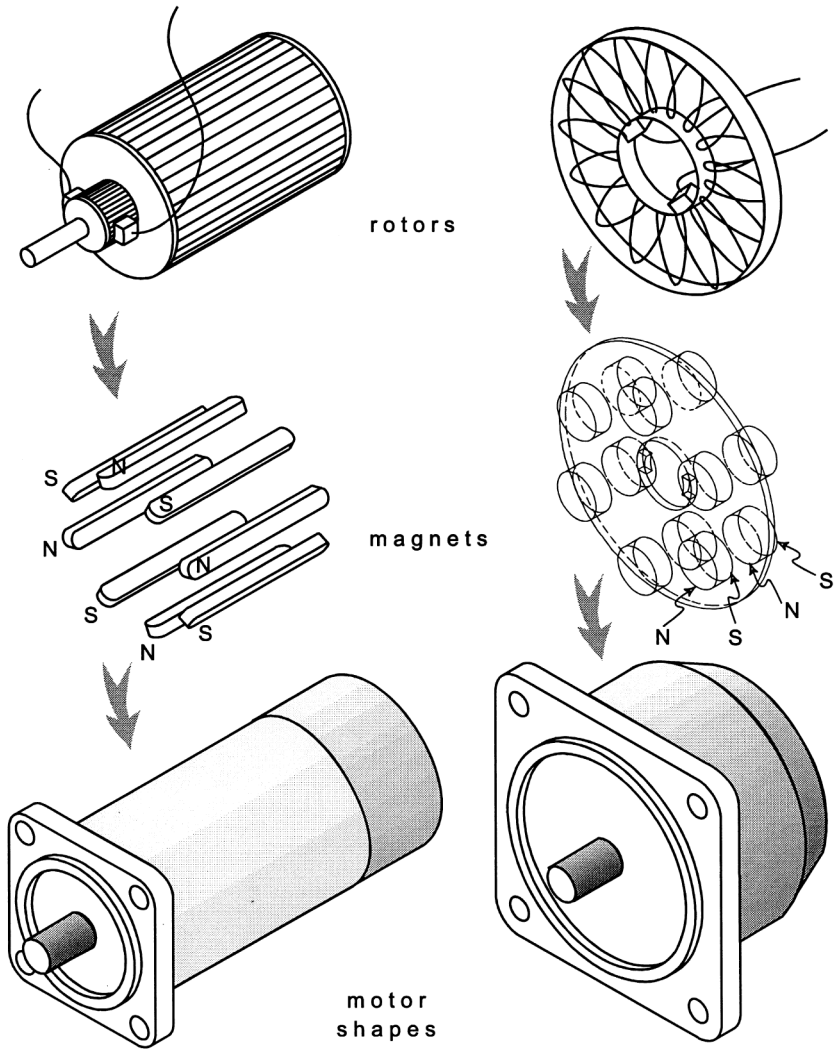

FIGURE 21.1 Different rotor shapes enable different overall shape of motors.

field and electrical circuit are needed. Accordingly, a motor has two parts, one carrying the magnets (we assume permanent magnets because they are most often used) and the other carrying the wire windings. The classical design means that magnets are placed on the static part of the motor (stator) while windings are on the rotary part (rotor). This concept understands brush-commutation. An advanced idea places magnets on the rotor and windings on the stator, and needs electronic commutation (brushless motors). The discussion starts with the classical design.

Permanent magnets create magnetic field inside the stator. If current flows through the windings (on rotor), force will appear producing a torque about the motor shaft. Figure 21.1 shows two rotor shapes, cylindrical and disc. Placement of magnets and finally the overall shape of the motor are also shown.

Let the angle of rotation be θ. This coordinate, together with the angular velocity $\dot{\theta}$, defines the rotor state. If rotor current is i, then the torque due to interaction with the magnetic field is $C_M i$. The constant C_M is known as the torque constant and can be found in catalogues. This torque has to solve several counter-torques. Torque due to inertia is $J\ddot{\theta}$, where J is the rotor's moment of

inertia and $\ddot{\theta}$ is angular acceleration. Torque that follows from viscous friction is $B\dot{\theta}$, where B is the friction coefficient. Values for J and B can be found in catalogues. Finally, the torque produced by the load has to be solved. Let the moment of external forces (load) be denoted by M. Very often this moment is called the output torque. Now, equilibrium of torques gives

$$C_M i = J\ddot{\theta} + B\dot{\theta} + M \tag{21.1}$$

To solve the dynamics of the electrical circuit we apply the Ohm's law. The voltage u supplied by the electric source covers the voltage drop over the armature resistance and counter-electromotive forces (e.m.f.):

$$u = Ri + C_E\dot{\theta} + Ldi / dt \tag{21.2}$$

Ri is the voltage drop where R is the armature resistance. $C_E\dot{\theta}$ is counter e.m.f. due to motion in magnetic field and C_E is the constant. Finally, Ldi/dt is counter e.m.f. due to self-inductance, where L is inductivity of windings. Values R, C_E, and L can be found in catalogues. The dynamics of electrical circuit introduces one new state variable, current i.

Equations (21.1) and (21.2) define the dynamics of the entire motor. If one wishes to write the dynamic model in canonical form, the state vector $x = [\theta\ \dot{\theta}\ i]^T$ should be introduced. Equations (21.1) and (21.2) can now be united into the form

$$\dot{x} = Cx + fM + du \tag{21.3}$$

The system matrices are

$$C = \begin{bmatrix} 0 & 1 & 0 \\ 0 & -B/J & C_M/J \\ 0 & -C_E/L & -R/L \end{bmatrix},\ f = \begin{bmatrix} 0 \\ -1/J \\ 0 \end{bmatrix},\ d = \begin{bmatrix} 0 \\ 0 \\ 1/L \end{bmatrix} \tag{21.4}$$

This is the third-order model of motor dynamics.

If inductivity L is small enough (it is a rather common case), the term Ldi/dt can be neglected. Equation (21.2) now becomes

$$u = Ri + C_E\dot{\theta} \tag{21.5}$$

and the number of state variables reduces to two. The state vector and the system matrices in eq. (21.3) are

$$x = \begin{bmatrix} \theta \\ \dot{\theta} \end{bmatrix},\ C = \begin{bmatrix} 0 & 0 \\ 0 & -C_M C_E / RJ - B/J \end{bmatrix},\ f = \begin{bmatrix} 0 \\ -1/J \end{bmatrix},\ d = \begin{bmatrix} 0 \\ C_M / R_J \end{bmatrix} \tag{21.6}$$

The motor control variable is u. By changing the voltage, one may control rotor speed or position.

If the motor drives a robot joint, for instance, joint j, we relate the motor with the joint by using index j with all variables and constants in the dynamic model (21.3). This was done in Section 20.3.1. when the motor model is integrated with the arm links model to obtain the dynamic model of the entire robot. There the second-order model in the form of Equations (21.1) and (21.5) was

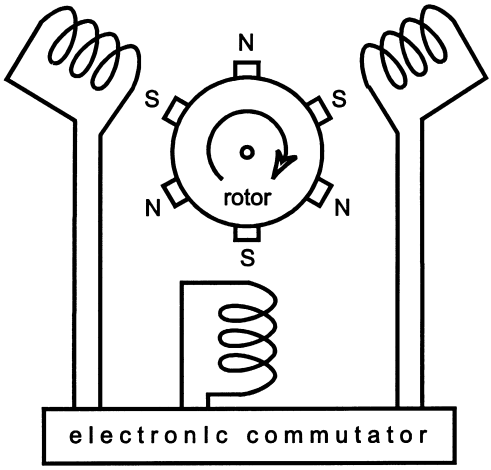

FIGURE 21.2 Scheme of brushless motor.

applied. If the third-order model is to be used, then the canonic form of motor dynamics, Equation (21.3), is combined with arm dynamics as explained in Section 20.3.2.

As already stated, the main disadvantage of the classical design of DC motors follows from brush-commutation. To avoid it, brushless motors place permanent magnets on the rotor and wire windings on the stator (Figure 21.2). The interaction between the magnetic field and the electrical circuit, which forces the rotor to move, still exists. Brushes are not needed because there is no current in the rotor. To synchronize switching in the electrical circuit and the angular velocity, Hall's sensors are used. They give the information for the device called an electronic commutator. In this way the electronic commutator imitates the brush commutation. We are not going to discuss the details of such a commutation system. Figure 21.2 shows the scheme of a brushless motor with three pairs of magnetic poles and three windings.

Let us briefly discuss the voltage supplied to the windings. It is a rectangular or trapezoidal signal switching between positive and negative values. Switching in a winding shifts with respect to the preceding winding. Because periods of constant voltage exist, we still deal with a DC motor. However, better performances can be achieved if a trapezoidal voltage profile is replaced with a sinusoidal one. In this case we have a three-phase AC supply, producing a rotating magnetic field of constant intensity. The magnetic force appears between the rotating field and the permanent magnets placed on the rotor, causing rotor motion. The rotating field pulls the rotor and they both rotate at the speed defined by the frequency of the AC signal. Changing the frequency, one may control the motor speed. This concept is called the synchronous AC motor. It is clear that the difference between a DC brushless motor and an AC synchronous motor is only in the supply.

21.1.3 How to Mount Motors to Robot Arms

When searching for the answer to the question posed in the heading, we face two criteria that conflict with each other. First, we prefer to use direct drive motors. They eliminate transmission and thus simplify arm construction and avoid backlash, friction, and deformation. Direct drive motors are used in robots, but not very often. Particularly, they are not appropriate for joints that are subject to a large gravitational load. The other criterion starts with the demand to unload the arm. With this aim, motors are displaced from the joints they drive. Motors are moved toward the robot base, creating better statics of the arm and reducing gravity in terms in joint torques. This concept introduces the need for a transmission mechanism that would connect a motor with the

corresponding joint. The presence of a transmission complicates the arm design (thus increasing the price) and introduces backlash (leading to lower accuracy when positioning some object), friction (energy loss due to friction and problems in controlling the system with friction), and elastic deformation (undesired oscillations). Despite all these drawbacks, some type of transmission is present in the majority of robots. It should be noted that the role of transmission is threefold. First, power is transmitted at distance. Second, speed can be reduced and torque increased if needed. Finally, it is possible to change the character of motion from the input to the output of transmission system: rotation to translation (R/T) or translation to rotation (T/R). If such change is not needed, the original character is kept: rotation (R/R) and translation (T/T). Here, we review some typical transmission systems that appear in robots, paying attention to the three mentioned roles of transmission.[3]

Spur gearing is an R/R transmission that has low backlash and high stiffness to stand large moments. It is not used for transmitting at a distance, but for speed reduction. One pair of gears has a limited reduction ratio (up to 10), and thus, several stages might be needed; however, the system weight, friction, and backlash will increase. This transmission is often applied to the first rotary arm axis. *Helical gears* have some advantages over spur gears. In robots, a large reduction of speed is often required. The problem with spur gears may arise from lack of an adequate gear tooth contact ratio. Helical gears have higher contact ratios and hence produce smoother output. However, they produce undesired axial gear loads. The mentioned gearing (spur and helical) is applied if the input and output rotation have parallel axes. If the axes are not parallel, then *bevel gearing* may be applied. An example of bevel gearing in a robot wrist is shown in Figure 21.7.

Worm gear allows a high R/R reduction ratio using only one pair. The main drawbacks are increased weight and friction losses that cause heat problems (e.g., efficiency less than 0.5).

Planetary gear is an R/R transmission used for speed reduction. The reduction ratio may be high but very often several stages are needed. Disadvantages of this system are that it is heavy in weight and often introduces backlash. So-called zero-backlash models are rather expensive. Note that buying a motor and a gearbox already attached to it and considering this assembly as one unit are recommended.

Harmonic drive is among the most common speed reduction systems in robots. This R/R transmission allows a very high reduction ratio (up to 300 and even more) using only one pair. As a consequence, compact size is achieved. Another advantage is small backlash, even near zero if selective assembly is conducted in manufacturing the device. On the other hand, static friction in these drives is high. The main problem, however, follows from the stiffness that allows considerable elastic deformation. Such torsion in joints may sometimes compromise robot accuracy.

Cyclo reducer is a R/R transmission that may increase the speed ratio up to 120 at one stage. As advantages, we also mention high stiffness and efficiency (0.75 to 0.85). The main drawbacks are heaviness and high price.

Toothed rack-and-pinion transmission allows R/T and T/R transformation of motion. In robots, R/T operation appears when long linear motion has to be actuated by an electric motor. The rack is attached to the structure that should be moved and motor torque is applied to the pinion (Figure 21.3a). The same principle may be found in robot grippers. T/R transmission can be applied if the hydraulic cylinder has to move a revolute joint. One example, actuation of rotary robot base, is shown in Figure 21.3b. Rack-and-pinion transmission is precise and inexpensive.

Recirculating ball nut and screw represent a very efficient R/T transmission. It also provides very high precision (zero backlash and high stiffness) and reliability along with great reduction of speed. A quality ball screw is an expensive transmission. One example of a ball screw applied in robots is presented in Figure 21.4. It is used to drive the vertical translation in a cylindrical robot.

Linkages and linkage structures may be considered transmission elements, although they are often structural elements as well. They feature very high stiffness and efficiency and small backlash. In Figure 21.5 a ball screw is combined with a linkage to drive the forearm of the ASEA robot.

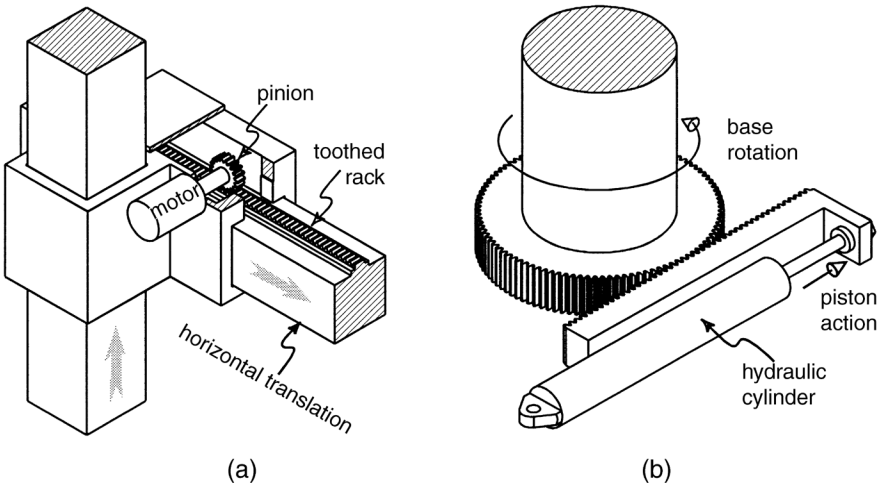

FIGURE 21.3 Toothed rack-and-pinion transmission.

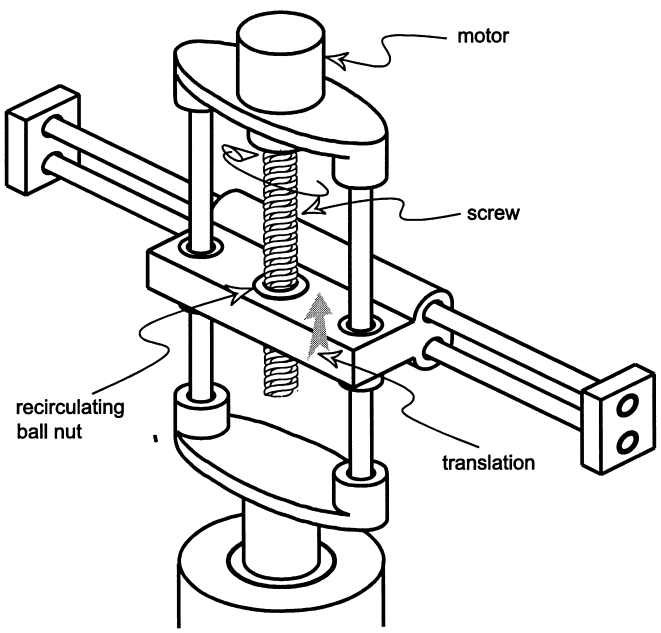

FIGURE 21.4 Application of ball screw transmission to vertical linear joint of a cylindrical robot.

Torsion shafts or torque tubes are R/R transmissions often used in robots to transmit power at a distance. They do not reduce speed. The problem of torsion deformation always exists with such systems. For this reason, it is recommended to transmit power at high speed (and low torque) because it allows smaller diameter and wall thickness, and lower weight. An example is shown in Figure 21.6. Wrist motors are located to create a counterbalance for the elbow. Motor power is transmitted to the wrist by means of three coaxial torque tubes.

Toothed belts can be found in low-cost robots. They are used to transmit rotary motion (R/R) at long distances. It is possible to reduce rotation speed, but it is not common. The usual speed ratio is 1:1. Toothed belt transmissions are very light in weight, simple, and cheap. The problems follow mainly from backlash and elastic deformation that cause vibrations. Figure 21.7 shows how the

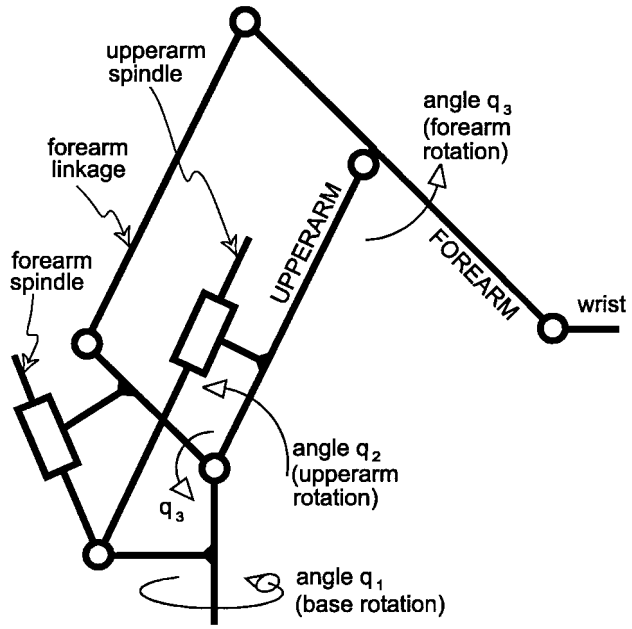

FIGURE 21.5 Ball screw combined with a linkage transmission.

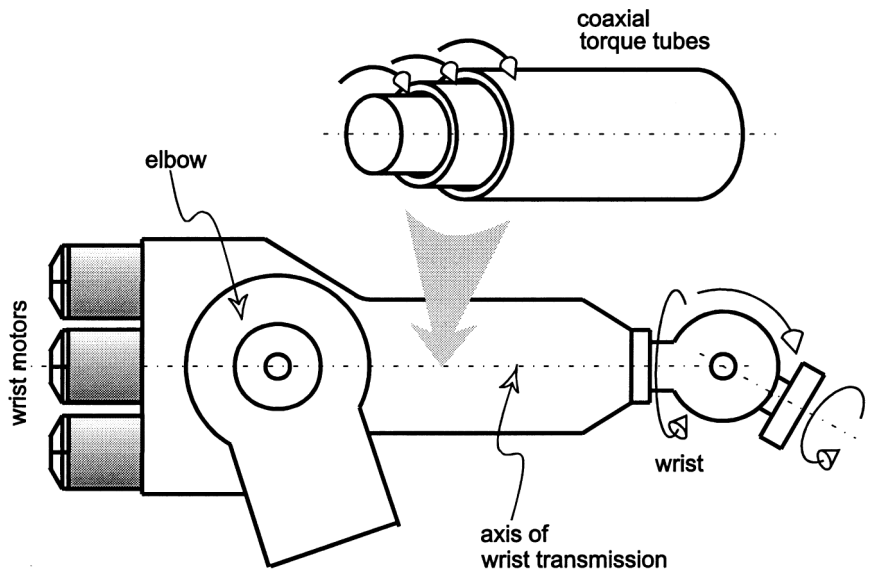

FIGURE 21.6 Wrist motors are used as a counterbalance and power is transmitted by means of coaxial torque tubes.

wrist can be driven by motors located at the robot base. Three belts are used for each motor to transmit power to the joint. In the wrist, bevel gearing is applied. The combined action of two motors can produce pitch and roll motion.

Chain drive can replace the toothed belt for transmitting rotary motion at a distance. It has no backlash and can be made to have stiffness that prevents vibrations. However, a chain transmission is heavy. Chain is primarily used as an R/R transmission, but sometimes it is applied for R/T and T/R operations.

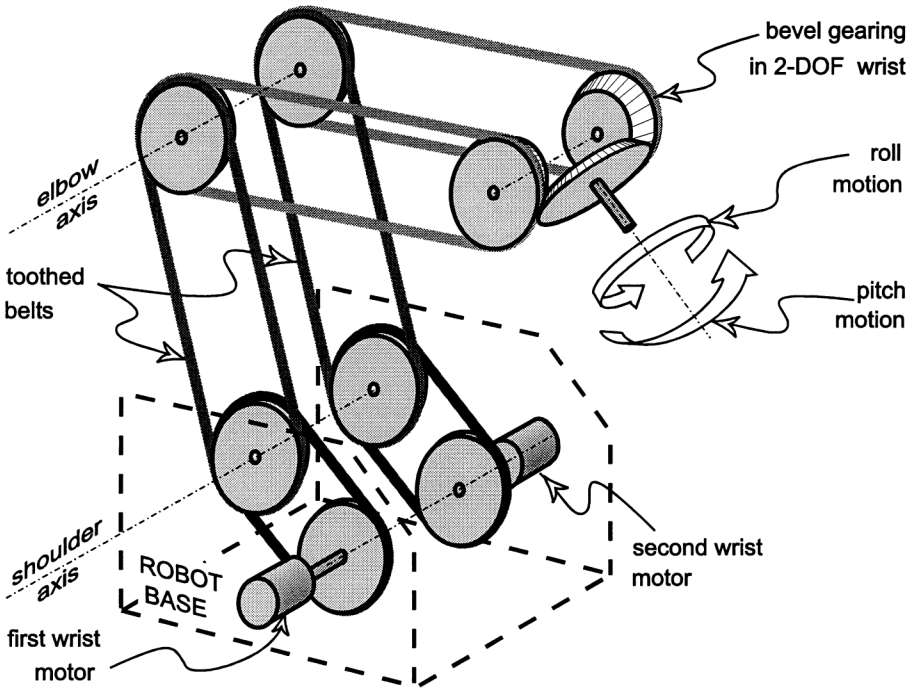

FIGURE 21.7 Motors driving the wrist are located at the robot base.

Mathematical model of transmission. Let us discuss the mathematical representation of transmission systems. If some actuator drives a robot joint, then motor motion θ and motor torque M represent the input for the transmission system. Joint motion q and joint torque τ are the output. An ideal transmission is characterized by the absence of backlash, friction, elastic deformation (infinite stiffness), and inertia. In modeling robot dynamics this is a rather common assumption. In such a case, there is a linear relation between the input and the output:

$$q = \theta/N, \tag{21.7}$$

$$\tau = MN \tag{21.8}$$

where N is the reduction ratio. This assumption allows simple integration of motor dynamics to the dynamic model of robot links.

However, transmission is never ideal. If backlash is present, relation (21.7) does not hold. Modeling of such a system is rather complicated, and hence, backlash is usually neglected. Friction is an always-present effect. Neglecting it would not be justified. It is well known that static friction introduces many problems in dynamic modeling. For this reason, friction is usually taken into account through power loss. We introduce the efficiency coefficient η as the output-to-input power ratio. Note that $0 < \eta < 1$. Now, Relation (21.8) is modified. If the motion is in the direction of the drive, then $N\eta'$ is used instead of N. However, if the motion is opposite to the action of the drive, then N/η'' is applied. Note that η' and η'' are generally different. The efficiency of a transmission in the reverse direction is usually smaller $\eta_j'' < \eta_j'$.

If transmission stiffness is not considered to be infinite, then the elastic deformation should be taken into account. Relation (21.7) does not hold since q and θ become independent coordinates. However, stiffness that is still high will keep the values q and θ/N close to each other. To solve the elastic deformation, one must know the values of stiffness and damping. The problem becomes even more complex if the inertia of transmission elements is not neglected. In that case, the

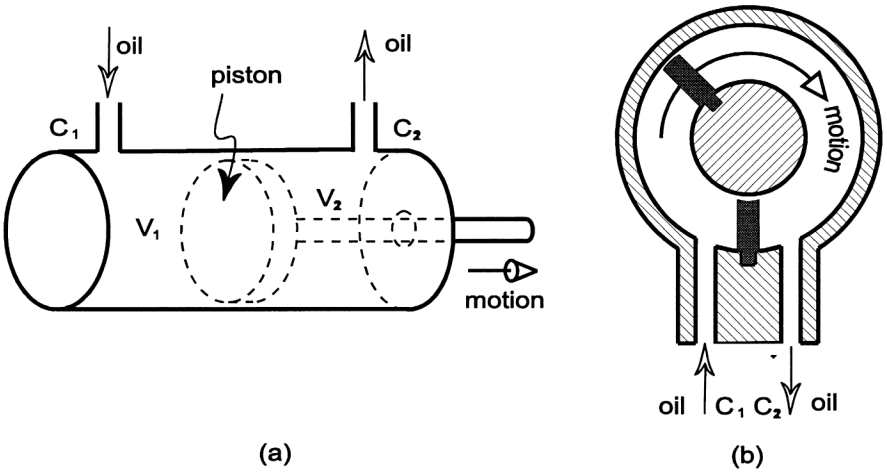

FIGURE 21.8 Hydraulic cylinder (a) and hydraulic vane motor (b).

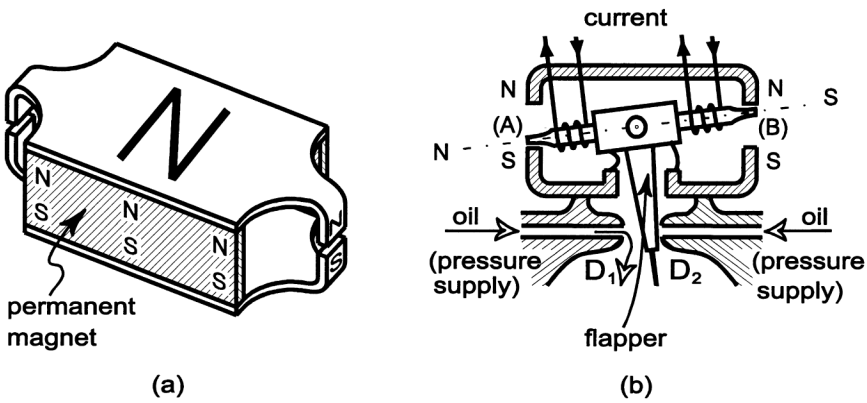

FIGURE 21.9 Torque motor: structure and operation.

transmission system requires dynamic modeling. One approach to this problem was presented in Section 20.5.4.

21.1.4 Hydraulic Actuators: Principles and Mathematics

Hydraulic servoactuator consists of a cylinder with a piston, a servovalve with a torque motor, an oil reservoir, and a pump. The term electrohydraulic actuator is also used. A reservoir and pump are necessary for the operation of the hydraulic system, but they are not essential for explaining operation principles. So, we restrict our consideration to the cylinder and the servovalve. The pump is seen simply as a pressure supply. A cylinder with a piston is shown in Figure 21.8a. If the pump forces the oil into port C_1, the piston will move to the right and volume V_1 will increase, V_2 will decrease and the oil will drain through port C_2. Oil flow and the difference in pressure on the two sides of the piston define the direction and speed of motion as well as the output actuator force. The same principle can be used to create a rotary actuator, a hydraulic vane motor (Figure 21.8b).

We explain the servovalve operation by starting with the torque motor (magnetic motor). The scheme of the motor is presented in Figure 21.9. If current flows through the armature windings as shown in Figure 21.9b, magnetic north will appear on side *A* and south on side *B*. Interaction

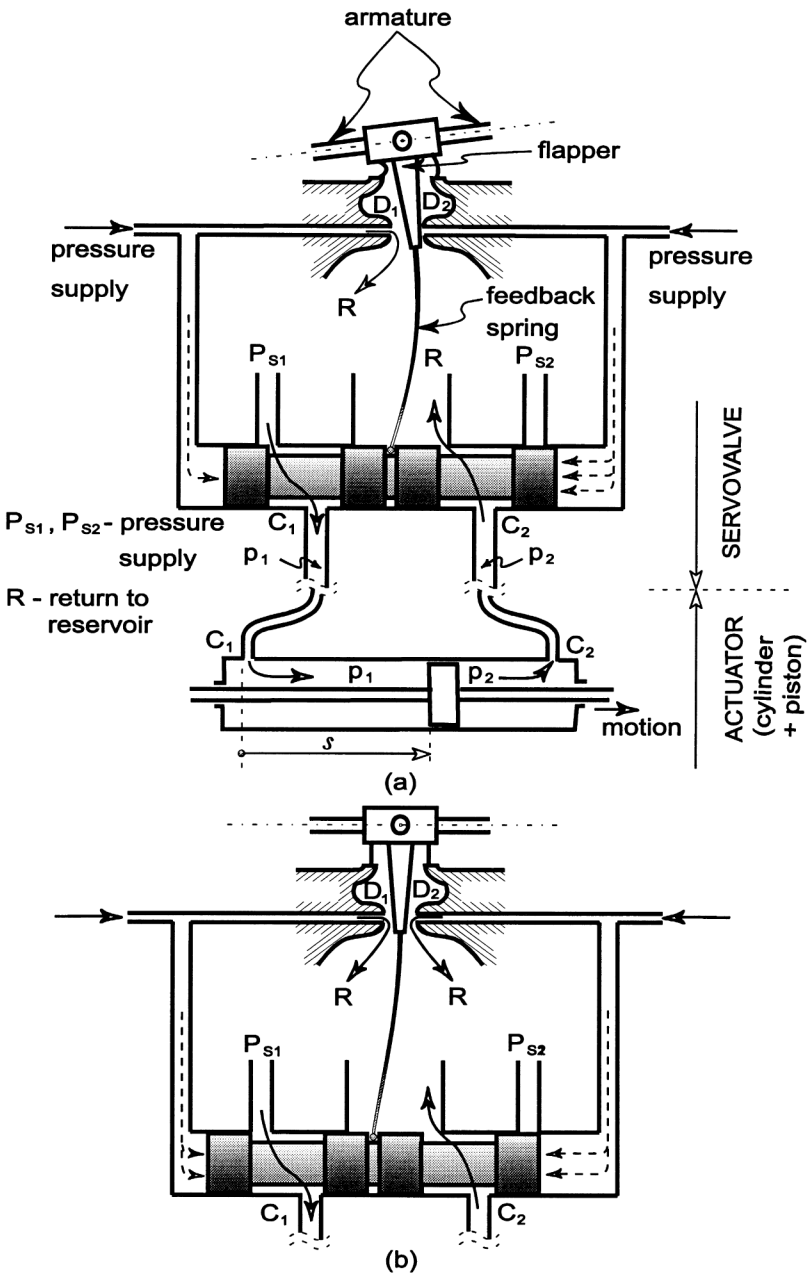

FIGURE 21.10 Operation of a servovalve.

with the permanent magnet will turn the armature to the left. Changing the current direction will turn the armature to the opposite side. When the armature moves, the flapper closes nozzle D_1 or D_2.

Figure 21.10 shows the complete servovalve. Let us explain how it works.[4] Suppose that current forces the armature to turn to the left (Figure 21.10a). The flapper moves to the right, thus closing nozzle D_2. The pressure supply line P_{s_2} is now closed and the oil from the left line, P_{s_1}, flows through pipe C_1 into the cylinder. The actuator piston moves to the right. Pipe C_2 allows the oil to flow out from the cylinder to the return line R (back to the reservoir). Since nozzle D_2 is closed,

the oil in the right supply line exerts strong pressure upon the right-hand side of the servovalve piston forcing it to move to the left. This motion causes deformation of the feedback spring. At some deformation, the elastic torque of the deformed spring starts to turn the armature to the right and the flapper to the left, thus opening nozzle D_2. When the oil begins to flow through D_2, the pressure acting upon the right-hand side of the piston reduces, but it is still stronger than the pressure acting upon the left-hand side. Hence, the piston continues moving to the left. The pressure on both sides of the servovalve piston balances when the flows through D_1 and D_2 become equal. This means the vertical position of the flapper, that is, the horizontal position of the armature (Figure 21.10b). The motion of the piston stops. In this position the motor torque equals the spring deformation torque. Let coordinate z define the position of the servovalve piston. The equilibrium of torques may be expressed by the relation

$$C_M i = \gamma z \tag{21.9}$$

where C_M is the motor torque constant, i is the armature current, γ is the coefficient of elastic deformation torque, and z expresses the magnitude of deformation. The equilibrium position z of the servovalve corresponds to some value of oil flow and accordingly some velocity of the piston in the actuator cylinder. Since current i can change the motor torque, and thus position z (according to Equation (21.9)), the possibility of controlling the flow and the actuator speed is achieved. Current i represents the control variable. One should note that after the change of the current, a transient phase takes place before the new equilibrium is established. However, one may neglect dynamics of the servovalve and avoid analysis of the transient phase. In such case, Equation (21.9) is satisfied all the time and thus servovalve position z immediately follows the changes of the current. The nonlinear static characteristic of the servovalve (flow depending on the pressure and the piston position) has the form

$$Q = Dwz\sqrt{\frac{1}{\rho}\left(p_s - \mathrm{sgn}(z)p_d\right)} \tag{21.10}$$

where p_s is the pressure in the supply line, $p_d = p_1 - p_2$ is the differential pressure, sgn(z) is the sign of the position coordinate z, ρ is the oil density, w is the area gradient of rectangular port (the rate of change of orifice area with servovalve piston motion), and D is a dimensionless coefficient. Differential pressure means the difference in pressures in pipes C_1 and C_2, and at the same time, the difference in pressure on the two sides of the actuator piston. For this reason it is often called the load pressure.

When modeling the dynamics of an actuator we assume, for simplicity, symmetry of the piston (Figure 21.11). Let coordinate s define the position of the actuator piston. The pressures on the two sides of the piston are p_1 and p_2, and hence, the oil exerts the force to the piston: $p_1A - p_2A = p_dA$, where A is the piston area. Dynamic equilibrium of forces acting on piston gives

$$p_dA = m\ddot{s} + B\dot{s} + F \tag{21.11}$$

where m is the mass (total mass of the piston and load referred to the piston), B is the viscous friction coefficient, and F is the external load force on the piston (often called the output force).

Consider now oil flow through a cylinder (Figure 21.11) and denote it by Q. It consists of three components. The first component follows from the piston motion. It is a product of piston area and velocity, $A\dot{s}$. The second component is due to leakage. Since leakage depends on pressure, we introduce leakage coefficient c as leakage per unit pressure. There are two kinds of leakage, internal and external, as shown in Figure 21.11. If the coefficient of internal leakage is c_i and that of the external is c_e, and if the coefficient of total leakage is defined as $c = c_i + c_e/2$, then the flow due to leakage is cp_d. Finally, the third component follows from oil compression. Its value is $(V/4\beta)\,\dot{P}_d$,

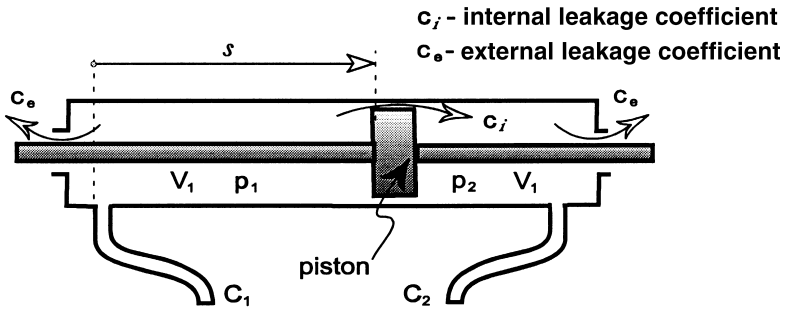

FIGURE 21.11 Oil flow through a hydraulic cylinder.

where V is the total volume ($V = V_1 + V_2$), and β is the compression coefficient. Total volume includes cylinder, pipes, and servovalve. Now, the flow is

$$Q = A\dot{s} + cp_d + \frac{V}{4\beta}\dot{p}_d \tag{21.12}$$

In this way we arrive at the mathematical model of the electrohydraulic actuator. The system dynamics is described by Equations (21.9) to (21.12). The model is nonlinear. The system state is defined by the three-dimensional vector $x = [s\ \dot{s}\ p_d]^T$. The control input is current i. The nonlinear model may be written in canonical form

$$\dot{x} = Cx + fF + d(x)i \tag{21.13}$$

where we tried to find analogy with the model (21.3) used for DC motors. Model matrices are

$$C = \begin{bmatrix} 0 & 1 & 0 \\ 0 & -B/m & A/m \\ 0 & -(4\beta/V)A & -(4\beta/V)c \end{bmatrix}, \quad f = \begin{bmatrix} 0 \\ -1/m \\ 0 \end{bmatrix},$$
$$d(x) = \begin{bmatrix} 0 \\ 0 \\ (4\beta/V)Dw(C_M/\gamma)\sqrt{(1/\rho)(p_s - \mathrm{sgn}(z)p_d)} \end{bmatrix} \tag{21.14}$$

If a linear model is required, the expression (21.10) should be linearized by expansion into a Taylor series about a particular operating point $K(z_K, p_{dK}, Q_K)$:

$$Q - Q_K = \left.\frac{\partial Q}{\partial z}\right|_K (z - z_K) + \left.\frac{\partial Q}{\partial p_d}\right|_K (p_d - p_{dK}) \tag{21.15}$$

The most important operating point is the origin of the flow-pressure curve ($Q_K = p_{dK} = z_k = 0$). In such a case relation (21.15) becomes

$$Q = k_1 z + k_2 p_d \tag{21.16}$$

where: $k_1 = \partial Q/\partial z$ and $k_2 = \partial Q/\partial p_d$ are called the valve coefficients. They are extremely important in determining stability, frequency response, and other dynamic characteristics. The flow gain k_1

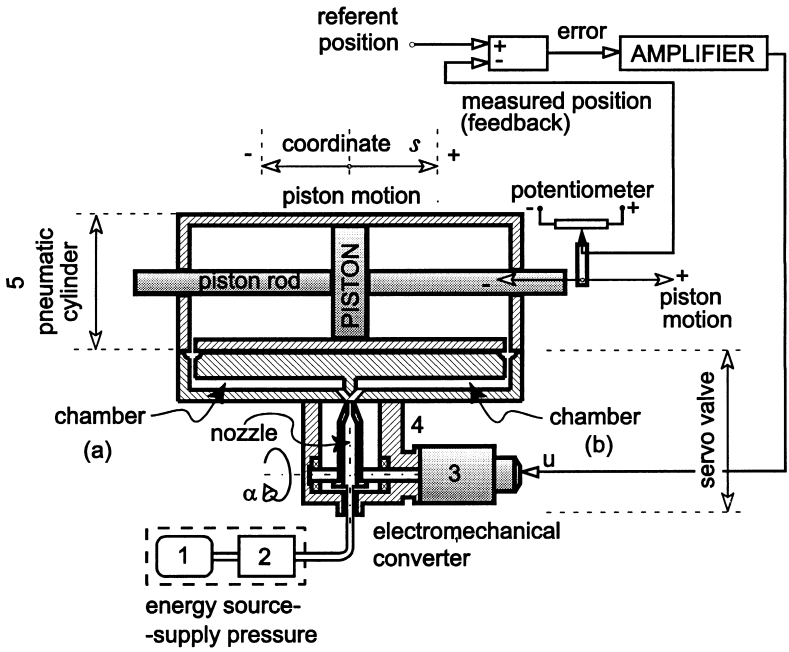

FIGURE 21.12 Scheme of a pneumatic servoactuator.

has a direct influence on system stability. The flow-pressure coefficient k_2 directly affects the damping ratio of valve–cylinder combination. Another useful quantity is the pressure sensitivity defined by $k_p = \partial p_d / \partial z = k_1 / k_2$. The pressure sensitivity of valves is quite high, which accounts for the ability of valve–cylinder combinations to break away large friction loads with little error. If (21.16) is used instead of (21.10), dynamic model (21.13) becomes linear with system matrices

$$C = \begin{bmatrix} 0 & 1 & 0 \\ 0 & -B/m & A/m \\ 0 & -(4\beta/V)A & (4\beta/V)(k_2 - c) \end{bmatrix}, \quad f = \begin{bmatrix} 0 \\ -1/m \\ 0 \end{bmatrix}, \quad d = \begin{bmatrix} 0 \\ 0 \\ (4\beta/V)k_1(C_M/\gamma) \end{bmatrix} \tag{21.17}$$

Model (21.13) in its linear or nonlinear form can be combined with arm dynamics, as explained in Section 20.3.2, to obtain the dynamic model of the complete robot system.

21.1.5 Pneumatic Actuators: Principles and Mathematics

A pneumatic servoactuator (often called a electropneumatic actuator) consists of an electropneumatic servovalve and a pneumatic cylinder with a piston. Figure 21.12 presents the scheme of the actuator. Let us explain how it operates.[5] Numbers 1 and 2 in the figure indicate an independent source of energy: (1) gas under pressure with (2) a valving and pressure reduction group. An electromechanical converter (3), a kind of torque motor, transforms the electrical signal (voltage u that comes from the amplifier) into an angle of its output shaft (angle α). The nozzle fixed to the shaft turns by the same angle. A mechanical-pneumatic converter (4) provides the difference in pressure and flow in chambers (a) and (b) proportional to the angle of the nozzle. The electromechanical converter and the mechanical-pneumatic converter together form the servovalve. The pneumatic cylinder (5) is supplied with differential pressure (p_d) and flow (Q_d), and hence, the piston moves. Thus, the voltage applied to the electromechanical converter represents the actuator-input variable that offers the possibility of controlling piston motion. Feedback is realized by using a sliding potentiometer (6). The potentiometer

provides for voltage proportional to piston displacement. This is analog information describing the position of the piston. The information is used to form the error signal by subtracting this position from the referent position. The error signal is amplified and then applied to the electromechanical converter. In this way the closed-loop control scheme is obtained.

Let us describe the dynamics of the pneumatic servoactuator mathematically. We first find the relation between the input and the output of the electromechanical converter. If the inductivity of the coil is neglected, the input voltage u reduces to:

$$u = R_c i \tag{21.18}$$

where R_c is the resistance of the circuit and i is the current. If the dynamics of the rotating parts (rotor, shaft, nozzle) is neglected, the output angle α will be proportional to the current:

$$\alpha = K_i i \tag{21.19}$$

where K_i is the coefficient of proportionality.

The flow through the mechanical-pneumatic converter is

$$Q_d = K_\alpha \alpha + K_p p_d \tag{21.20}$$

where p_d is the differential pressure (in two chambers), K_α is the flow gain coefficient with respect to angle α, and K_p is the flow gain coefficient with respect to pressure.

Now we consider the cylinder. Let the coordinate s define the position of the piston. Flow through the pneumatic cylinder can be described by the relation

$$Q_d = \frac{M p_s \zeta A}{R T_s} \dot{s} + \frac{M V_0}{k R T_s} \dot{p}_d \tag{21.21}$$

where M is the molecular mass of gas, p_s is the supply pressure, ζ is the pressure-loss coefficient, R is the universal gas constant, T_s is the supply temperature, A is the active piston area, k is the polytropic exponent, V_0 is the total volume. Dynamic equilibrium of forces acting on piston gives

$$p_d A = m\ddot{s} + B\dot{s} + F \tag{21.22}$$

where m is the total piston mass (including rod and other load referred to the piston), B is the viscous friction coefficient, and F is the external load force on the piston (often called the output force). Note that there may exist other forces like dry friction (F_{fr} sgn $\dot{s}$) or linear force (cs). In such cases Equation (21.22) has to be augmented.

Equations (21.18) to (21.22) describe the dynamics of the electropneumatic actuator. If the equations are rearranged, canonical form of the dynamic model can be obtained. The system state is defined by the three-dimensional vector $x = [s\ \dot{s}\ p_d]^T$. The control variable is voltage u. Equations (21.18) to (21.22) can be united in the linear matrix model

$$\dot{x} = Cx + f F + du \tag{21.23}$$

where model matrices are

$$C = \begin{bmatrix} 0 & 1 & 0 \\ 0 & -B/m & A/m \\ 0 & -p_s \zeta A k / V_0 & R T_s k K_p / M V_0 \end{bmatrix}, \quad f = \begin{bmatrix} 0 \\ -1/m \\ 0 \end{bmatrix}, \quad d = \begin{bmatrix} 0 \\ 0 \\ R T_s k K_\alpha K_i / M V_0 R_c \end{bmatrix} \tag{21.24}$$

Model (21.23) can be combined with the arm dynamics, as explained in Section 20.3.2, to obtain the dynamic model of the complete robot system.

It should be said that electropneumatic servosystems cannot be applied practically for servodrives of robotic manipulators. This is because all gases to be applied as driving media are compressible, i.e., their specific volume is pressure dependent. In this way elasticity is introduced into the driving system. Under a load, especially in cases of longer strokes, large loads, and big pneumatic cylinders, this phenomenon leads to oscillations of loaded links of manipulator chain, thus rendering the electropneumatic drives practically unusable for robotic servodrives. This is a real situation present on the market and industry today. Pneumatic drives are applied in simple pick-and-place industrial systems positioned by mechanical stops.

The other variants of driving units need more extensive presentation.

21.2 Computer-Aided Design

As the number of industrial robots used in manufacturing systems increases and robots tend to be used in many nonindustrial fields, additional functions and performance improvements, such as high speed motion and high precision positioning, are desirable. It is, however, difficult to design robots by the conventional method of experimentation and trial manufacturing because robots involve many design parameters and evaluation functions. Accordingly, computer-aided design (CAD) is significant for designing suitable robots for objective tasks and saving manpower, time, and costs required for design.

21.2.1 Robot Manipulator Design Problem

Designing a robot manipulator (or robot) requires a determination of all design parameters of its mechanism.

- Fundamental mechanism:
  1. Degrees of freedom (D.O.F.)
  2. Joint types (rotational/sliding)
  3. Arm lengths and offsets
- Inner mechanism:
  1. Motor allocations
  2. Types of transmission mechanisms
  3. Motors
  4. Reduction gears and their reduction ratios
  5. Arm cross-sectional dimensions
  6. Machine elements

The designed robot should have suitable functions and abilities to perform certain tasks. The following design functions must be evaluated:

- Kinematic evaluation:
  1. Workspace
  2. Joint operating range
  3. Maximum workpiece velocity and acceleration
  4. Maximum joint velocity and acceleration
- Static/dynamic evaluation:
  1. Maximum motor driving torque
  2. Total motor power
  3. Total weight

TABLE 21.1 Relationship between Design Parameters and Evaluation Functions

	Evaluation Function											
	Kinematics				Dynamics						Both	
Design Parameter	Workspace	Joint Disp. Limit	Max. Joint Vel./Acc.	Max. Workpiece Vel./Acc.	Max. Motor Torque	Total Motor Power	Total Weight	Weight Capacity	Deflection	Natural Frequency	Positioning Accuracy	Cost
Fundamental Mechanism												
D.O.F.	∀	Δ	Δ	Δ	Δ	○	○	Δ	○	○	○	∀
Joint type	∀	○	Δ	Δ	Δ	○	○	Δ	○	○	○	∀
Arm length	∀	Δ	∀	∀	∀	∀	∀	∀	∀	∀	∀	○
Offset	∀	∀	Δ	Δ	Δ	Δ	Δ	○	Δ	Δ	Δ	Δ
Inner Mechanism												
Motor allocation	Δ	Δ	Δ	Δ	∀	∀	∀	∀	Δ	Δ	Δ	Δ
Trans. mech.	Δ	∀	Δ	Δ	Δ	Δ	∀	Δ	∀	∀	∀	∀
Motor	Δ	Δ	∀	∀	∀	∀	∀	∀	Δ	Δ	Δ	∀
Reduction gear	Δ	Δ	∀	∀	∀	∀	∀	∀	∀	∀	∀	∀
Arm cross. dim.	Δ	Δ	Δ	Δ	∀	Δ	∀	∀	∀	∀	∀	○
Machine element	Δ	Δ	Δ	Δ	∀	Δ	∀	∀	∀	∀	∀	○

∀ = strong, ○ = medium, Δ = weak.

Source: Modified from Inoue, K., et al., *J. Robotics Soc. Jpn.*, 14, 710, 1996. With permission.

4. Weight capacity
5. Maximum deflection
6. Minimum natural frequency

The relationship between design parameters and evaluation functions is shown in Table 21.1. It shows that kinematics strongly depends on fundamental mechanism, while dynamics depends on inner mechanism.

Many robot CAD systems have been developed throughout the world.[6-18] Among them is TOCARD (total computer-aided robot design), which has the ability to design robots comprehensively and will be explained later.

21.2.2 Robot Design Procedure

Figure 21.13 shows the total robot design procedure in this CAD system. First, the operator (designer) inputs the design conditions which are prescribed by the objective tasks. Then, the procedure consists of three design systems — *fundamental mechanism design, inner mechanism design,* and *detailed structure design*, described as follows:

1. Fundamental mechanism design is based on kinematic evaluation — workspace, joint displacement, velocity and acceleration, and workpiece velocity and acceleration.
2. Inner mechanism design requires determination of motor allocations and the types of transmission mechanisms. The arm cross-sectional dimensions are calculated roughly, and the machine elements including the motors and the reduction gears are selected from their catalog data temporarily, based on rough evaluation of dynamics — motor driving torque, total motor power, total weight, weight capacity, and deflection.
3. Detailed structure design involves modification of the arm cross-sectional dimensions and reselection of the machine elements based on precise evaluation of dynamics — total weight, deflection, and natural frequency.

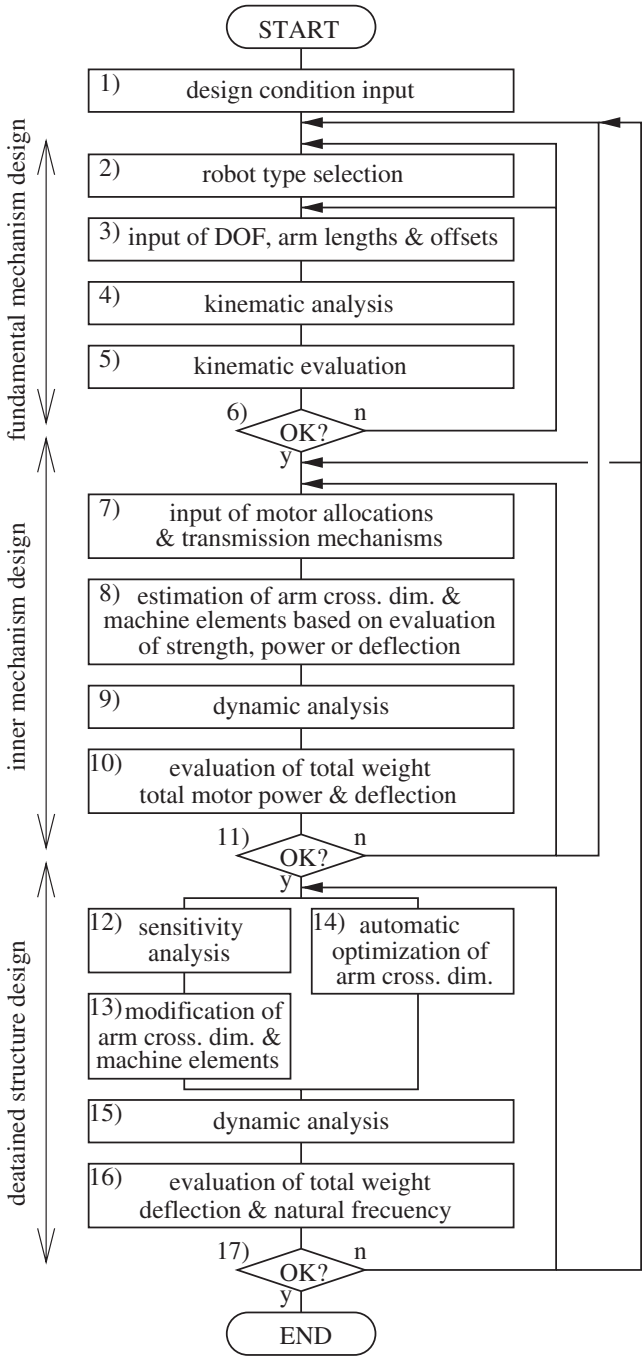

FIGURE 21.13 Total robot design procedure in TOCARD. (Modified from Inoue, K. et al., *J. Robotics Soc. Jpn.*, 14, 710, 1996. With permission.)

Some of the design parameters are locally optimized in each system. However, if sufficient performance cannot be obtained in a system, the operator returns back to the previous system and tries the previous design again. The CAD system is an interactive design system; the operator can repeatedly alternate between design change and evaluation. The details of the above-mentioned design systems are described in the following sections.

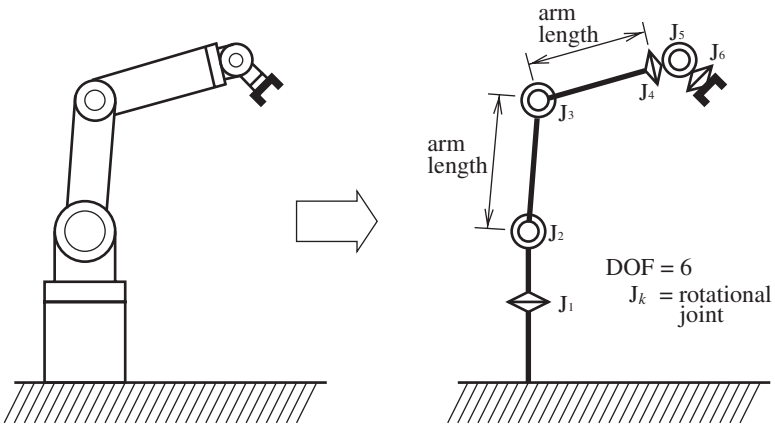

FIGURE 21.14 Fundamental mechanism of robot.

21.2.3 Design Condition Input

21.2.3.1 Step 1

The operator inputs the design conditions or constraints prescribed by the objective tasks:

1. Sizes and weights of workpieces (including end-effectors)
2. Reference trajectories of workpieces
3. Required working space
4. Allowable deflection and natural frequency

21.2.4 Fundamental Mechanism Design

The kinematic design parameters of a robot that is a serial link mechanism as shown in Figure 21.14, are called the "fundamental mechanism:"

1. Degrees of freedom
2. Joint types (rotational/sliding)
3. Arm lengths and offsets

The fundamental mechanism is determined based on kinematic evaluation.

21.2.4.1 Step 2

The type of robot mechanism — how rotational or sliding joints are serially arranged — is called robot type, and most industrial robots are classified into the following categories:

- Cartesian robot (or rectangular robot)
- Cylindrical robot
- Spherical robot (or polar robot)
- Articulated robot
- SCARA robot

Generally, a robot design expert selects a suitable robot type for the objective tasks from these categories, using empirical knowledge concerning the characteristics of the performance of each robot type. Here a new method is introduced for selecting the most suitable robot type for the tasks from the typical six-D.O.F. industrial robot types based on rough evaluation of the performances using fuzzy theory. In this method, the performances of robot types derived from the design expert's knowledge are roughly compared with the performances required for the tasks

using fuzzy theory.[19] The method is outlined below, where the italics in the examples are expressed using fuzzy sets.

1. Five performances, workspace, dexterity, speed, accuracy, and weight capacity, are evaluated in robot type selection, in the same way as a robot design expert's method. These and the suitability for the objective tasks of a robot type are expressed by fuzzy sets.
   Example 21.1: Workspace is *large*.
   Example 21.2: Suitability for task is *very high* (*very suitable* for task).
2. The empirical knowledge of the design expert concerning performance of each robot type is expressed in the form of a fact. All such knowledge is stored in the system beforehand.
   Example 21.3: Workspace of articulated robot is *very large*.
3. The operator analyzes the tasks and obtains the performances required for them, which are expressed as a set of rules; these rules are input by the operator.
   Example 21.4: If workspace of robot type is *large*, it is *suitable* for painting task.
   Example 21.5: If workspace of robot type is *small*, it is *never suitable* for painting task.
4. The suitability of each robot type for the tasks is obtained from 2 and 3 above by fuzzy reasoning (Mamdani's method).
   Example 21.6: Articulated robot is *very suitable* for painting task.
5. After the suitabilities of all robot types are obtained, the operator selects the most suitable type.

21.2.4.2 Step 3

After the robot type is selected, the operator inputs and modifies arm lengths and offsets. He can also add new joints or can remove the joints that do not move when the robot moves along the reference trajectories given as the design condition, thus increasing/reducing degrees of freedom.

21.2.4.3 Step 4

Once the fundamental mechanism is determined using the above two steps, then kinematic analyses are applied to the designed mechanism.

Forward kinematics (Figure 21.15) — Forward kinematics calculates the workpiece position and orientation $\boldsymbol{R}$ from the joint displacement vector $\boldsymbol{q}$. Transformation matrix is often used for the forward kinematics of a serial link manipulator; this system uses the revised transformation matrix of the Denavit–Hartenberg method.[20]

Inverse kinematics (Figure 21.15) — An efficient algorithm of inverse kinematics problem calculating $\boldsymbol{q}$ from $\boldsymbol{R}$ was developed by Takano.[20] This algorithm is applicable to all types of a six-DOF robot with three rotational joints in the wrist and can obtain a maximum eight sets of solutions. Inverse kinematics is used for calculating the joint trajectories $\boldsymbol{q}[t]$ corresponding to the workpiece reference trajectories $\boldsymbol{R}[t]$ given as the design condition.

Workspace analysis (Figure 21.15) — Evaluating the workspace generated by three joints near the base is sufficient for the robot design. The method developed by Inoue can efficiently obtain the boundary surface of such workspace of any type of robot, considering the joint operating range.[21]

Velocity/acceleration analysis (Figure 21.16) — Luh's algorithm[22] includes the process calculating the workpiece velocity **v** and acceleration **a** from $\boldsymbol{q}$, $\dot{\boldsymbol{q}}$, and $\ddot{\boldsymbol{q}}$; it is used here.

21.2.4.4 Step 5

Kinematic performances of the designed fundamental mechanism are evaluated by:

- The workspace considering the joint operating range must cover the required working space for the objective tasks given as the design condition (Figure 21.15).
- The joint operating range is limited by the structure of the joint. While wide joint operating range makes workspace large, a long sliding joint makes the robot heavy, and using a

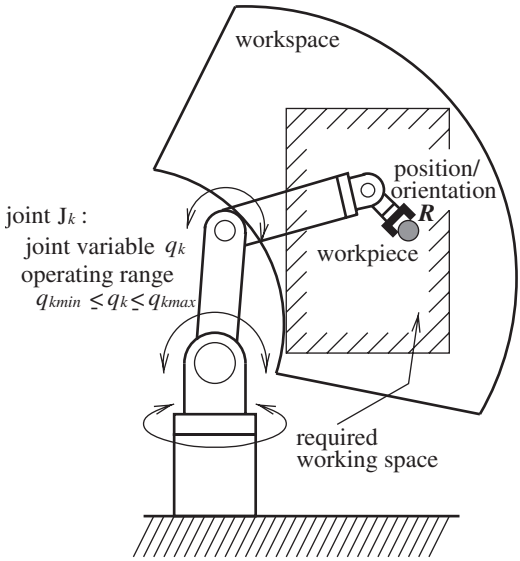

FIGURE 21.15 Position kinematics, workspace, and joint operating range.

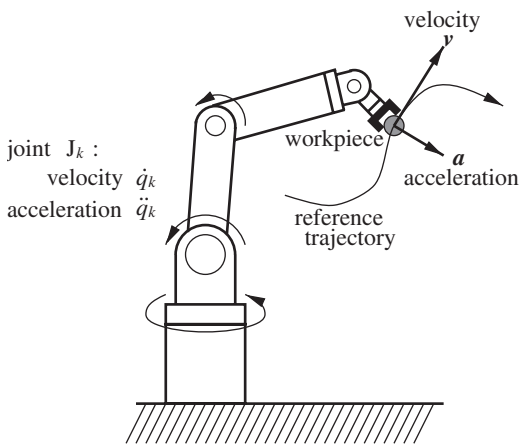

FIGURE 21.16 Workpiece velocity/acceleration and joint velocity/acceleration.

rotational joint with offset reduces the stiffness of the joint shaft to radial force. Thus, the joint operating range is evaluated as described above (Figure 21.15).

- The maximum workpiece velocity and acceleration required for the objective tasks are given indirectly as the design condition — the reference trajectories of workpieces (Figure 21.16).
- The maximum joint velocity and acceleration on the given trajectories should be as small as possible so that the robot can be moved by small and light motors (Figure 21.16).

21.2.4.5 Step 6

The operator repeats the design change and evaluation alternately in Steps 3 through 5. If the above interactive design fails, the operator goes back to Step 2 and selects another suitable robot type. This procedure is repeated until the suitable fundamental mechanism is obtained.

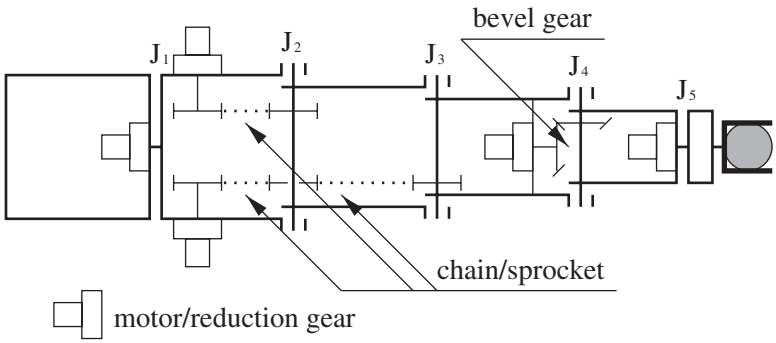

FIGURE 21.17 Joint driving systems of robot. (Modified from Inoue, K. et al., *J. Robotics Soc. Jpn.*, 14, 710, 1996. With permission.)

21.2.5 Inner Mechanism Design

The following design parameters are called "inner mechanism:"

1. Motor allocations (where the motors are to be attached)
2. Types of transmission mechanisms
3. Motors
4. Reduction gears and their reduction ratio
5. Arm cross-sectional dimensions
6. Machine elements (bearings, chains, bevel gears, etc.)

In the inner mechanism design, (1) and (2) are determined, (5) is calculated roughly, and (3), (4), and (6) are selected from catalog data temporarily, based on rough evaluation of dynamics — motor driving torque, total motor power, total weight, weight capacity, and deflection.

21.2.5.1 Step 7

As shown in Figure 21.17, a joint driving system consists of an actuator, a reduction gear, and transmission mechanisms (if needed). Five types of driving elements used in this CAD system are

1. Motor/reduction gear element
2. Shaft element
3. Chain/sprocket element
4. Bevel gear element
5. Ball screw/nut element

We adopted motors and harmonic drives as actuators and reduction gears respectively, because these are used in many industrial robots in the present time. Direct drive motors can be modeled as motor/reduction gear elements without reduction gears. Ordinary belts and timing belts are dealt with as chain/sprocket elements, because they are the same as chains kinematically, and only have different stiffnesses and weights. In this step, the operator inputs motor allocations and types of transmission mechanisms, as illustrated in Figure 21.18.

21.2.5.2 Step 8

Five types of arm/joint elements are used here (Figure 21.19).

1. Cylindrical arm element
2. Prismatic arm element
3. Revolute joint element (type 1)
4. Revolute joint element (type 2)
5. Sliding joint element

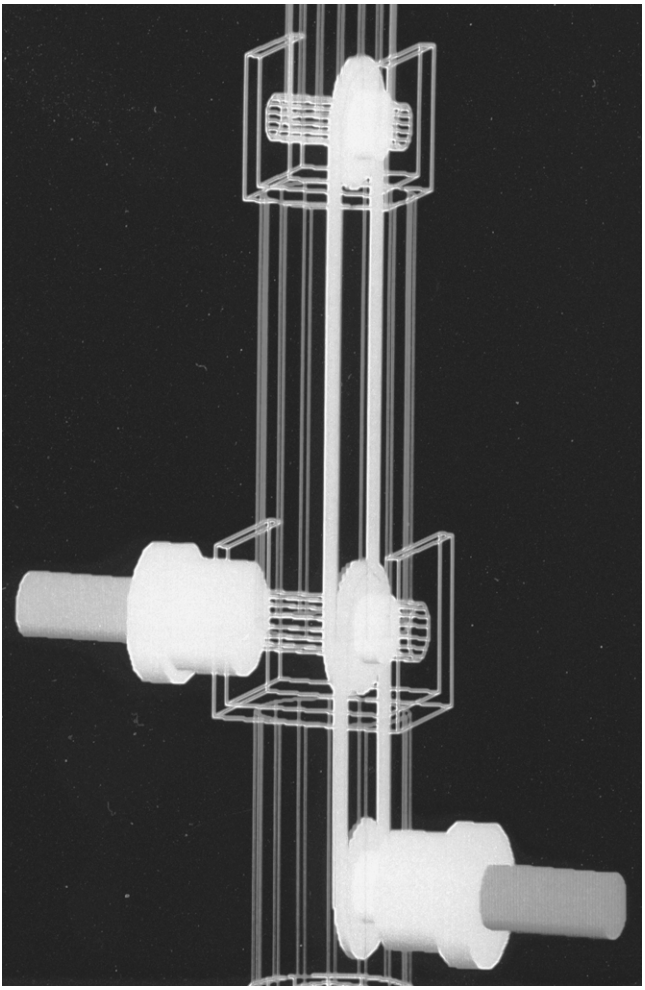

FIGURE 21.18 Example of designed transmission mechanisms. (From Inoue, K. et al., *J. Robotics Soc. Jpn.*, 14, 710, 1996. With permission.)

Because the arm cross-sectional dimensions of arm elements, the bearings used in joint elements, and the machine elements used in driving elements are design parameters, the system roughly calculates arm cross-sectional dimensions and selects motors, reduction gears, and machine elements (bearings, chains, bevel gears, etc.) from catalog data temporarily. This is done so that each arm, joint, or driving element will have enough strength and stiffness against the internal force acting on it and each motor will have enough power and torque to move the robot. In Figure 21.20, B_i is the i-th arm element, and $\boldsymbol{f}_i$ is the force/moment acting on the lower arm element B_{i-1} from B_i. If the joint element J_i is rotational, the moment around the joint axis of $\boldsymbol{f}_i$ is the joint driving torque τ_i of J_i; if J_i is sliding, the force in the joint axis direction of $\boldsymbol{f}_i$ is the joint driving force, which is converted into τ_i with the ball screw/nut element.

1. The cross-sectional dimension of the arm element B_i is determined to minimize the weight of B_i under the constraint that its deflection to the maximum value of the force/moment $\boldsymbol{f}_{i+1}$ acting on B_i from the upper arm element B_{i+1} is less than its allowable deflection.
2. The weight, the position of center of gravity, and the inertia tensor of B_i are calculated from the determined dimension.

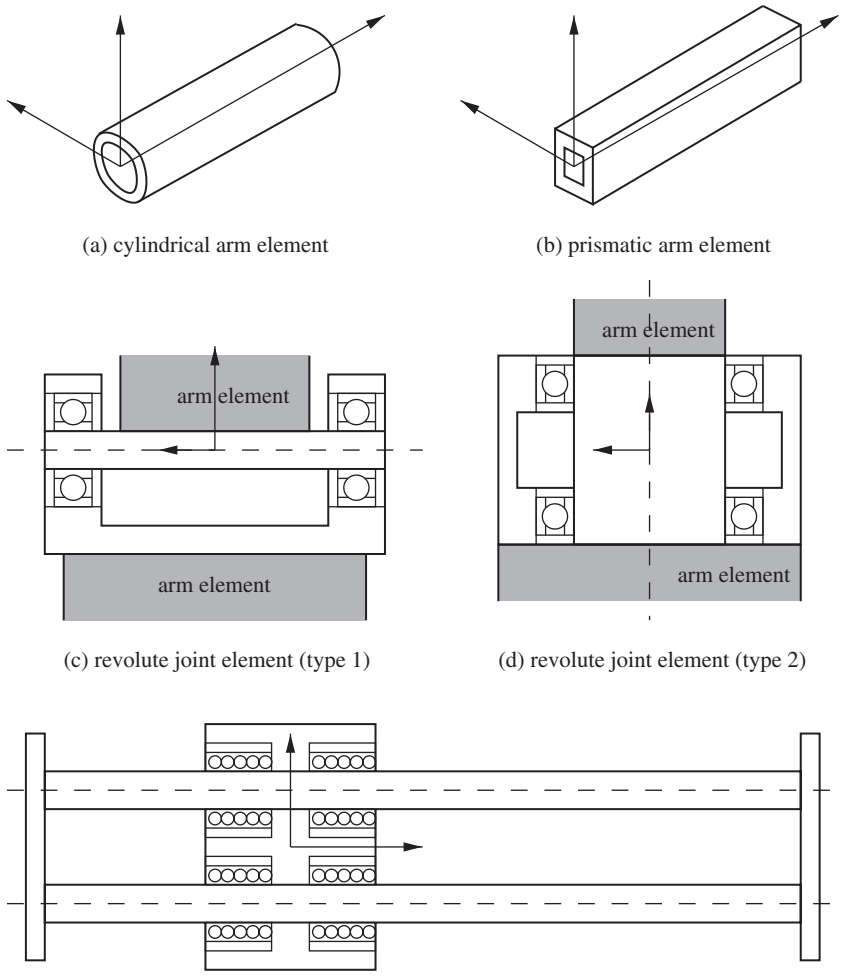

(a) cylindrical arm element

(b) prismatic arm element

(c) revolute joint element (type 1)

(d) revolute joint element (type 2)

(e) sliding joint element

FIGURE 21.19 Arm/joint elements. (Modified from Inoue, K. et al., *J. Robotics Soc. Jpn.*, 14, 710, 1996. With permission.)

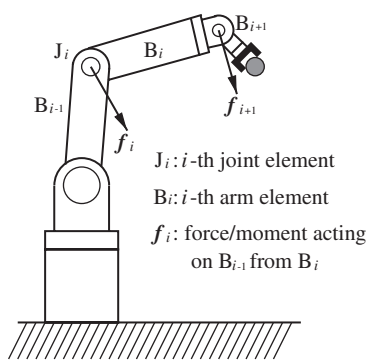

FIGURE 21.20 Automatic design of each element in inner mechanism design.

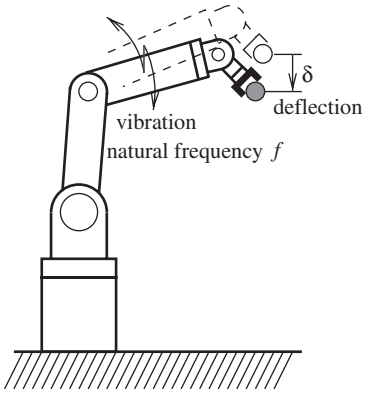

FIGURE 21.21 Deflection and natural frequency.

3. The force/moment $\boldsymbol{f}_i$ acting on the lower arm element B_{i-1} from B_i, thus the joint driving torque τ_i, can be obtained via the inverse dynamics of B_i along the trajectories given as the design condition.
4. The bearing used in the joint element J_i is selected from the catalog data so that the bearing may be lightest and have greater allowable radial/thrust load than the maximum value of $\boldsymbol{f}_i$.
5. Each machine element used in the transmission mechanism of J_i is selected from the catalog data so that it may be lightest and have greater allowable torque than the maximum value of τ_i.
6. The reduction ratio of the reduction gear for J_i is determined via mechanical impedance matching.*
7. The motor driving J_i is selected from the catalog data so that it may be lightest and have enough rated power and allowable torque to move J_i.
8. Repeating the above-mentioned procedure alternately from the tip arm element to the base arm element allows us to determine the design parameters of the elements temporarily.

21.2.5.3 Step 9

Determining all design parameters of the robot temporarily in this way permits the following dynamic analyses.

Inverse dynamics — We expanded Luh's algorithm so that it can be applied to robots with transmission mechanisms as shown in Figure 21.17; the revised method can calculate both the joint driving torque τ and the motor driving torque τ_m when the robot motion $\boldsymbol{q}$, $\dot{\boldsymbol{q}}$, and $\ddot{\boldsymbol{q}}$ are given. This method can also calculate the internal force/moment $\boldsymbol{f}_i$ acting on each arm element, which is used in design of each element as described above.

Deflection analysis (Figure 21.21) — Generally, the stiffness of bearings in joints, reduction gears, and transmission mechanisms is not negligible because it is less than the stiffness of arms. Thus we developed an elastic model of a robot by the finite element method (FEM), which is applicable to robots with transmission mechanisms and deals with the stiffness of arms as well as that of bearings, reduction gears, and transmission mechanisms.[23,24] Using this model, we calculate the deflection δ when the robot motions $\boldsymbol{q}$, $\dot{\boldsymbol{q}}$, and $\ddot{\boldsymbol{q}}$ are given.

21.2.5.4 Step 10

The operator evaluates the dynamic performances of the designed robot:

Maximum motor driving torque — The maximum motor driving torque on the trajectories given as the design condition should be as small as possible in order to use small and light motors.

*When the moment of inertia of motor and arm are I_m and I_a, reduction ratio $n = \sqrt{I_a / I_m}$ gives the maximum arm acceleration by the constant motor torque. It is called "mechanical impedance matching."

Total motor power — Total motor power required for the robot to do the objective tasks should be as small as possible, leading to low cost.

Total weight — The total weight of the robot should also be as small as possible, to reduce cost. Lightening the robot enables high speed motion and makes the transportation and installation of the robot easy.

Weight capacity — The robot must have enough weight capacity to carry the workpieces dealt with in the objective tasks. This constraint is given as a design condition — the weight of workpieces.

Maximum deflection — Deflection strongly depends on the balance of the stiffness and weight of the robot, and the deflection affects the accuracy. The maximum deflection on the given trajectories should be nearly equal to the allowable deflection given as the design condition. The constraint on the deflection will be evaluated again in the detailed structure design.

21.2.5.5 Step 11

If sufficient performance cannot be obtained in Step 10, the operator returns to Step 7 and changes the motor allocations and the types of transmission mechanisms. Steps 7–10 are repeated until the suitable motor allocations and the suitable types of transmission mechanisms for the objective tasks are obtained.

21.2.6 Detailed Structure Design

The arm cross-sectional dimensions and/or machine elements, which have already been locally optimized on each element in the inner mechanism design, are modified/reselected to minimize the total weight under the constraints that the deflection is lower than the allowable deflection and that the natural frequency is higher than the allowable frequency:

$$\begin{cases} \text{objective function} & = & m \rightarrow \min \\ \text{constraints} & = & \delta \le \delta_0, \quad f \ge f_0 \end{cases} \tag{21.25}$$

where m = total weight, δ = maximum deflection of robot at the point of grasped workpiece, f = natural frequency of the first vibration mode of robot, δ_0 = allowable deflection given as design condition, and f_0 = allowable natural frequency given as design condition.

The above-mentioned global optimization is important to attain both high speed motion and high precision positioning. This optimization problem can be rewritten into the objective function Q to be minimized:

$$Q \equiv m + \frac{w_d}{\delta_0^2}\left\{\max(0,\ \delta - \delta_0)\right\}^2 + \frac{w_f}{f_0^2}\{\max(0, f_0 - f)\}^2 \rightarrow \min, \tag{21.26}$$

where $w_d(>0)$ = penalty for deflection constraint and $w_f(>0)$ = penalty for natural frequency constraint.

δ_0, f_0, w_d, and w_f are input by the operator as the design conditions. Steps 12, 13, and 14 help the operator determine the arm cross-sectional dimensions and the machine elements.

21.2.6.1 Steps 12 and 13

Letting the parameter p_i be one of the arm cross-sectional dimensions and machine elements, the sensitivity S_i of p_i is defined by:

$$s_i \equiv \delta Q / \delta p_i \tag{21.27}$$

Obviously, the most sensitive parameter (the parameter with negative, and the smallest, sensitivity) is most effective for minimizing Q. In Step 12, the system calculates all sensitivities of the

TABLE 21.2 Workpiece Allowable Deflection, and Allowable Natural Frequency Given as Design Conditions

Length of workpiece		100.0 mm
Weight of workpiece		2.0 kg
Allowable deflection	δ_0	0.5 mm
Allowable natural frequency	f_0	25.0 Hz
Penalty for deflection	w_d	10000.0 kg
Penalty for frequency	w_f	10000.0 kg

Source: From Inoue, K., et al., *J. Robotics Soc. Jpn.*, 14, 710, 1996. With permission.

arm cross-sectional dimensions and the machine elements. Then, in Step 13, the operator selects and modifies the most sensitive parameter.

21.2.6.2 Step 14

The system calculates the optimal arm cross-sectional dimensions which minimize Q under the constraints on their allowable ranges by the gradient projection method.

21.2.6.3 Step 15

In addition to deflection analysis, we perform natural frequency analysis (Figure 21.21). The natural frequency f for the given joint displacement $\boldsymbol{q}$ (the given pose of robot) is calculated by FEM, using the elastic model used in deflection analysis.

21.2.6.4 Step 16

The operator evaluates the total weight, maximum deflection, and minimum natural frequency according to Equation (21.25).

- The total weight should be minimized.
- The maximum deflection on the given trajectories must be less than the allowable deflection.
- Natural frequency also depends on the balance of the stiffness and weight of the robot, and low natural frequency causes low accuracy because of residual vibration after positioning. The minimum natural frequency on the given trajectories must be higher than the allowable natural frequency.

21.2.6.5 Step 17

The above-mentioned design change and evaluation, Steps 12 through 16, are repeated alternately until the optimal arm cross-sectional dimensions and machine elements are obtained; then the robot design is terminated.

21.2.7 Design Example

The design conditions are summarized in Table 21.2 and Figures 21.22 and 21.23. Figure 21.24 shows the robot designed by the above-mentioned procedure, and Tables 21.3 through 21.5, summarize its main design parameters. Furthermore, Figures 21.22, 21.23, 21.25 and Table 21.6 show the various performances of the designed robot. Figure 21.26 illustrates the change in the total weight, deflection, and natural frequency with repetition of design change in the detailed structure design. As shown here, we could have reduced the total weight with a few repetitions, keeping the deflection and the natural frequency within the allowable ranges given as the design conditions. The robot finally obtained is about 1.1 kg lighter than that obtained temporarily with the inner mechanism design.

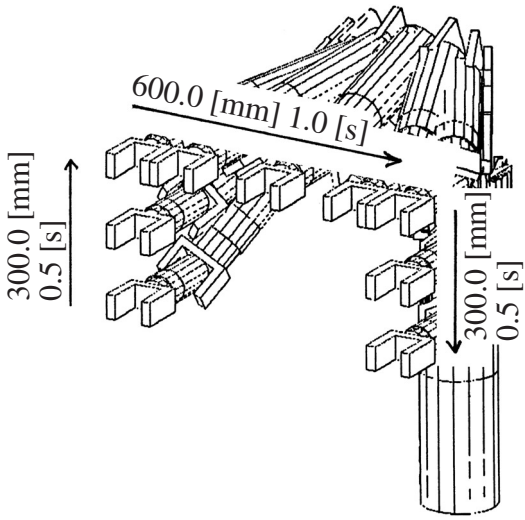

FIGURE 21.22 Trajectory given as design condition and animation of designed robot moving along it. (From Inoue, K. et al., *J. Robotics Soc. Jpn.*, 14, 710, 1996. With permission.)

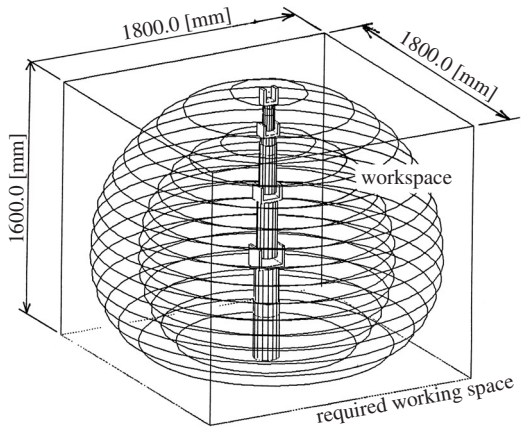

FIGURE 21.23 Required working space given as design condition and workspace of designed robot. (From Inoue, K. et al., *J. Robotics Soc. Jpn.*, 14, 710, 1996. With permission.)

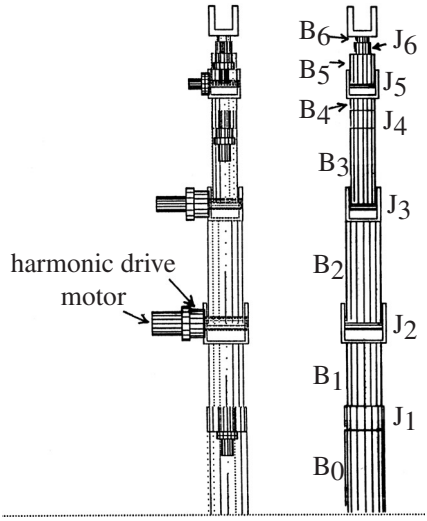

FIGURE 21.24 Designed robot using TOCARD. (From Inoue, K. et al., *J. Robotics Soc. Jpn.*, 14, 710, 1996. With permission.)

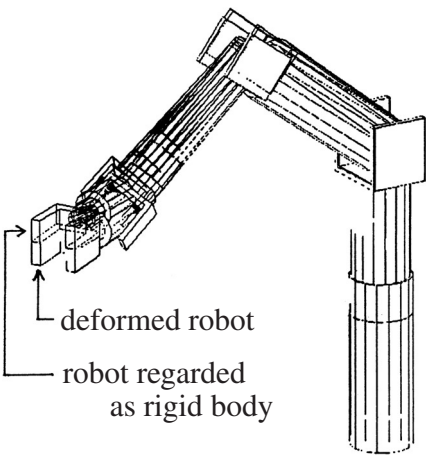

FIGURE 21.25 Maximum deflection (0.468 mm) on given trajectory of designed robot. (From Inoue, K. et al., *J. Robotics Soc. Jpn.*, 14, 710, 1996. With permission.)

TABLE 21.3 Arm Parameters of Designed Robot

Arm	Length (mm)	Diameter (mm)	Thickness (mm)
B_0	320.0	130.0	9.0
B_1	320.0	120.0	10.0
B_2	400.0	120.0	2.0
B_3	280.0	84.0	2.0
B_4	120.0	84.0	2.0
B_5	120.0	84.0	2.0
B_6	40.0	44.5	2.0
Total	1600.0		

Cylindrical arm element (Duralumin).

Source: From Inoue, K., et al., *J. Robotics Soc. Jpn.*, 14, 710, 1996. With permission.

TABLE 21.4 Joint Parameters of Designed Robot

Joint	Type	Distance between Bearings (mm)	Bearing Internal Diameter (mm)
J_1	(b)	80.0	6812 (60.0)
J_2	(a)	140.0	6809 (45.0)
J_3	(a)	106.0	6807 (35.0)
J_4	(b)	60.0	6808 (40.0)
J_5	(a)	100.0	6804 (20.0)
J_6	(b)	40.0	6805 (25.0)

(a) = Revolute (type 1) joint element; (b) = revolute (type 2) joint element.

Source: From Inoue, K., et al., *J. Robotics Soc. Jpn*, 14, 710, 1996. With permission.

TABLE 21.5 Joint Driving System Parameters of Designed Robot

Motor Joint	Rated Power (W)	Harmonic Drive (Reduction Ratio)
J_1	L402-011 (23.0)	FRS-20-160 (160)
J_2	L720-012 (200.0)	CSS-32-160 (160)
J_3	L511-012 (110.0)	CSS-32-160 (160)
J_4	L402-011 (23.0)	CSS-20-80 (80)
J_5	R301-011 (11.0)	FRS-20-160 (160)
J_6	R301-011 (11.0)	CSS-20-50 (50)

The motor and harmonic drive are directly attached to their joint axis.

Source: From Inoue, K., et al., *J. Robotics Soc. Jpn.*, 14, 710, 1996. With permission.

TABLE 21.6 Performance Parameters of Designed Robot

Parameter	Performance
Total motor power	378.0 W
Total weight	24.0 kg
Maximum deflection on given trajectory	0.468 mm
Minimum natural frequency on given trajectory	25.0 Hz

Source: Modified from Inoue, K., et al., *J. Robotics Soc. Jpn.*, 14, 710, 1996. With permission.

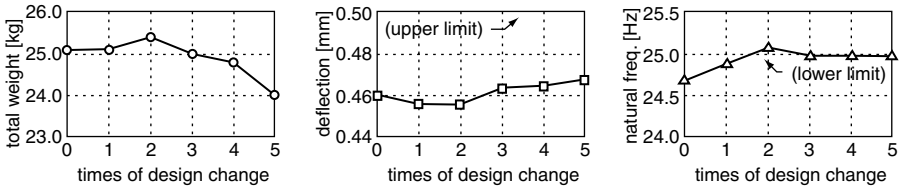

FIGURE 21.26 Change in total weight, deflection, and natural frequency with iteration of design change in detailed structure design. (From Inoue, K. et al., *J. Robotics Soc. Jpn.*, 14, 710, 1996. With permission.)

References

1. Vukobratović, M., and Potkonjak, V., *Dynamics of Manipulation Robots: Theory and Application*, *Sci. Fundam. Robotics,* Springer Verlag, Berlin, 1982.
2. Vukobratović, M. and Stokić, D., *Control of Manipulation Robots, Theory and Application*, Springer Verlag, Berlin, 1982.
3. Nof, S.Y. (Ed.), *Handbook of Industrial Robotics,* John Wiley & Sons, New York, 1985.
4. Merit, H.E., *Hydraulic Control Systems,* John Wiley & Sons, New York, 1967.
5. Vukobratović, M., *Applied Dynamics of Manipulation Robots,* Springer Verlag, Berlin, 1989.
6. Chedmail, P., Robot structures and actuators optimization, *Proc. 16th Int. Symp. Ind. Robots*, 185, 1986.
7. Erdman, A.G., Thompson, T., and Riley, D.R., Type selection of robot and gripper kinematic topology using expert system, *Int. J. Robotics Res.*, 5(2), 183, 1986.
8. Fenton, R.G. and Lipitkas, J., Optimum design of manipulators, *Comput.-Aided Eng. Robotics*, 68, 1984.
9. Gosselin, C.M. and Guillot, M., The synthesis of manipulators with prescribed workspace, *ASME J. Mech. Design*, 113, 451, 1991.
10. Kim, J. and Khosla, P.K., A formulation for task based design of robot manipulators, *Proc. 1993 IEEE/RSJ Int. Conf. Intelligent Robots Syst.*, 2310, 1993.
11. Lin, C.D., and Freudenstein, F., Optimization of the workspace of a three-link turning-pair connected robot arm, *Int. J. Robotics Res.*, 5(2), 104, 1986.
12. Paden, B., Optimal kinematic design of 6R manipulators, *Int. J. Robotics Res.*, 7(2), 43, 1988.
13. Paredis, C.J.J. and Khosla, P.K., Kinematic design of serial link manipulators from task specifications, *Int. J. Robotics Res.*, 12(3), 274, 1993.
14. Potkonjak, V., Vukobratović, M., and Hristic, D., Interactive procedure for computer-aided design of industrial robots mechanisms, *Proc. 13th Int. Symp. Ind. Robots*, 16, 1983.
15. Potkonjak, V. and Vukobratović, M., Computer-aided design of manipulation robots via multiparameter optimization, *Mechanism and Machine Theory*, 18(6), 431, 1983.

16. Vukobratović, M., and Potkonjak, V., Applied Dynamics and CAD of Manipulation Robots, *Sci. Fundam. Robotics*, Springer Verlag, Berlin, chap. 6, 1985.
17. Vijaykumar, R., Waldron, K.J., and Tsai, M.J., Geometric optimization of serial chain manipulator structures for working volume and dexterity, *Int. J. Robotics Res.*, 5(2), 91, 1986.
18. Yang, D.C.H. and Lee, T.W., Heuristic combinatorial optimization in the design of manipulator workspace, *IEEE Trans. SMC*, 14(4), 571, 1984.
19. Inoue, K., Takano, M., and Sasaki, K., Type selection of robot manipulators using fuzzy reasoning in robot design system, *Proc. 1993 IEEE/RSJ Int. Conf. Intelligent Robots Sys.*, 926, 1993.
20. Takano, M., A new effective solution for inverse kinematics problem (synthesis) of a robot with any type of configuration, *J. Fac. Eng. Univ. Tokyo*(*B*), 38(2), 107, 1985.
21. Inoue, K., Takano, M., and Sasaki, K., Development of robot CAD system (5th report) calculation method of workspace using inverse kinematics, *Proc. 1989 JSPE* (*Autumn*), 279, 1989, (in Japanese).
22. Luh, J.Y.S., Walker, M.W., and Paul, R.P.C., On-line computational scheme for mechanical manipulators, *ASME J. Dynamic Syst., Meas., Control*, 102, 69, 1980.
23. Inoue, K., Takano, M., and Sasaki, K., Optimum design of robot manipulators using sensitivity analysis, *Proc. 20th Int. Symp. Ind. Robots*, 513, 1989.
24. Inoue, K., Takano, M., and Sasaki, K., Optimal design system of robot structures using sensitivity to dynamical characteristics, *J. Robotics Soc. Jpn.*, 9(1), 18, 1991 (in Japanese).